Electronic Supplementary Material (ESI) for Soft Matter.

Electronic Supplemental Information for Drop on a bent fibre

Zhao Pan, Floriane Weyer, William G. Pitt, Nicolas Vandewalle & Tadd T. Truscott

Table of Contents

1 Restless Night: a Chinese poem about droplet formation and detachment

竹凉侵卧内，野月满庭隅。

As bamboo chill drifts into the bed room, moon light fills every corner of our garden.

重露成涓滴，稀星乍有无。

Heavy dew beads and trickles, stars suddenly there, sparse, next aren't.

暗飞萤自照，水宿鸟相呼。

Fireflies in dark flight flash, waking water birds begin calling, one to another.

万事干戈里，空悲清夜徂!

All things caught between shield and sword, All grief empty, the clear night passes.

[1] Tu F, Hinton D (1989) The selected poems of Tu Fu. (New Directions Publishing).

2 Supplemental figures

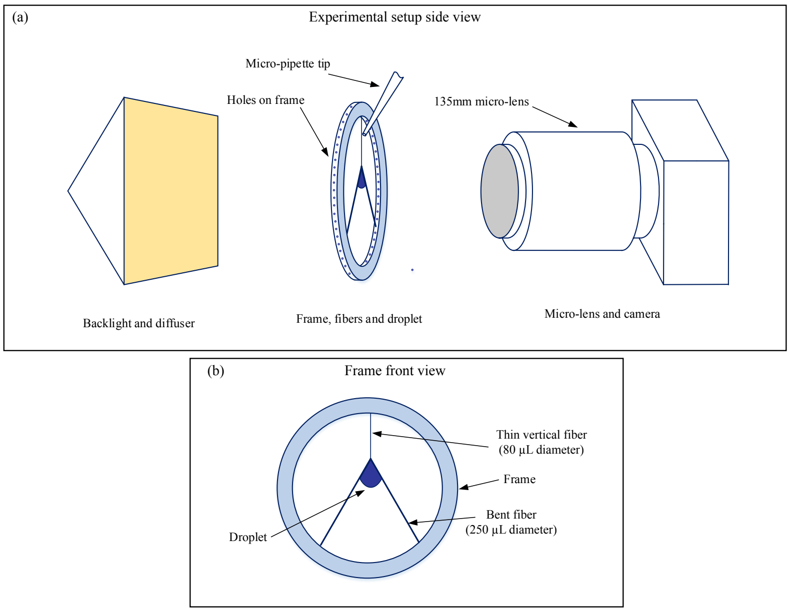

Fig. S1: Side and front view of a 3D printed frame used in the experiments. A 250 µm thick fibre attached on the frame is stretched and bent by an 80 µm vertical fibre. An SDS solution droplet is attached on the bent fibre by means of a micro-pipette tip. A camera photographs the droplet using a backlight.

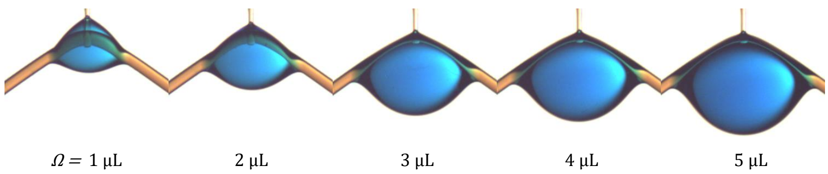

Fig. S2: SDS-water solution droplets of different volumes attached to a fibre ($\theta = 54.59°$). The vertical thin fibre affected the profile of the droplet by wicking liquid upward via capillary force. However, when a droplet is large ($\Omega > 3$ µL) the contribution due to wicking is negligible.

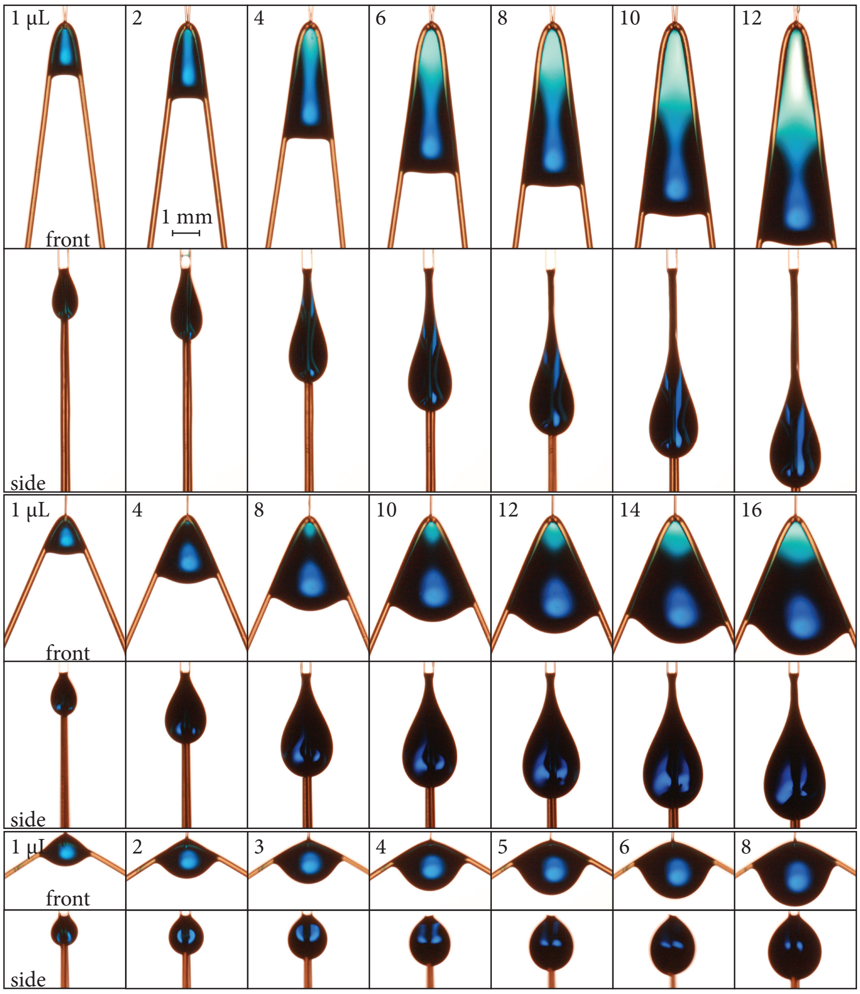

Fig. S3: Front and side views of SDS-water solution droplets of increasing volumes (Ω) attached to fibres with three different half-angles (Ω).

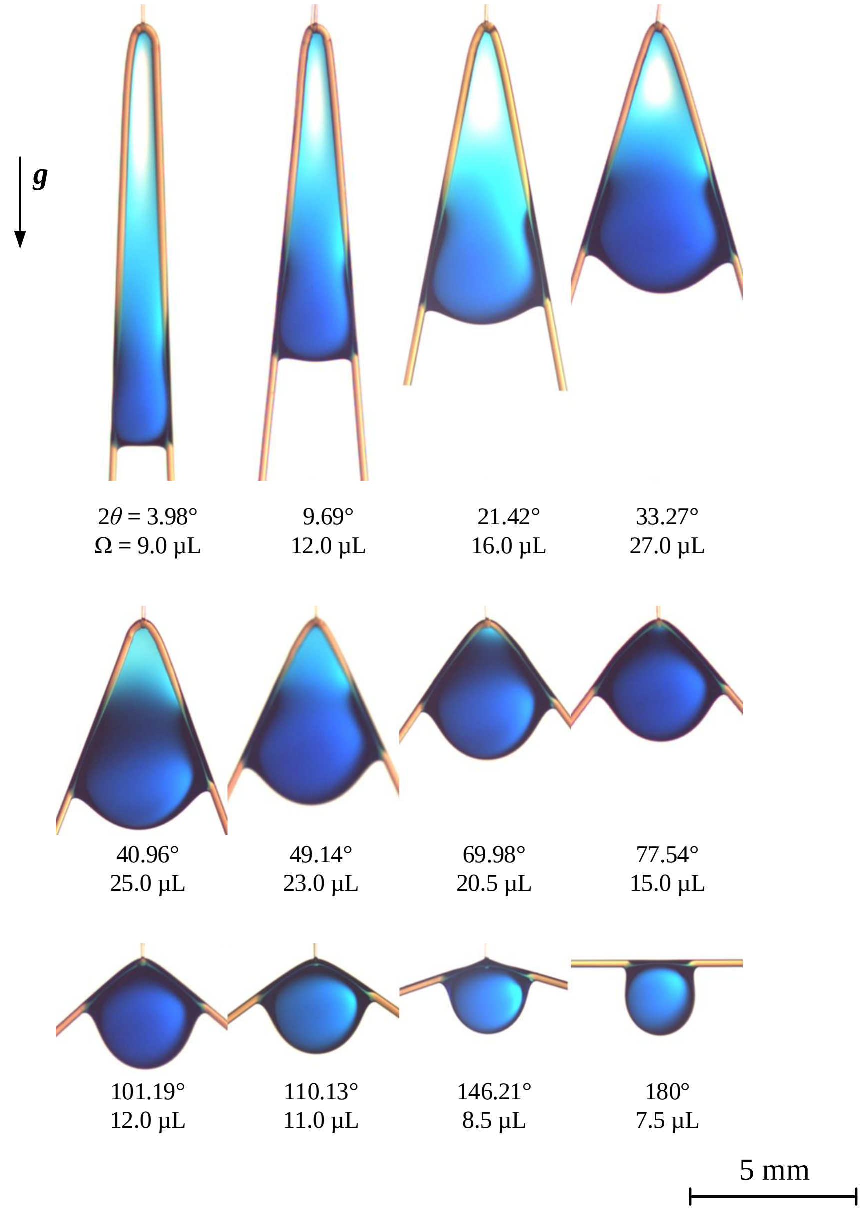

Fig. S4: The critical droplet volumes (Ω) of an SDS-water solution for a given θ, as examples of specific data points in Figs. 2, 4 & 5.

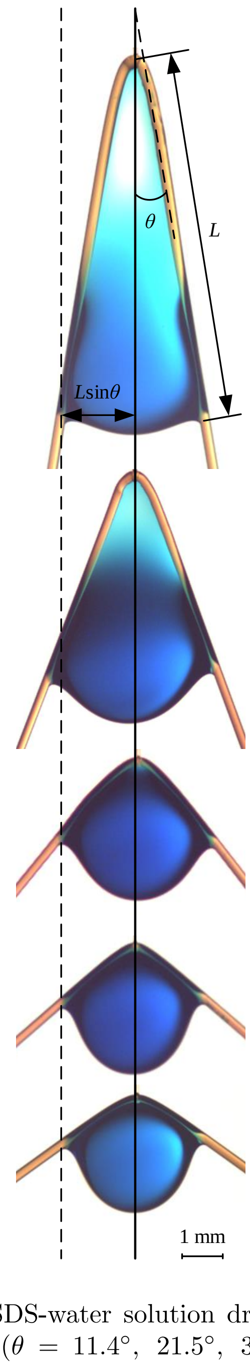

Fig. S5: Photographs of SDS-water solution droplets at critical state on fibre bent to various angels (θ = 11.4°, 21.5°, 39.7°, 49.5°, 54.5° and Ω = 20, 25, 15, 12.5, 11 µL from top to bottom).

3 Supplemental video captions

SI_video_1.avi: High speed video of an SDS-water solution droplet (14 µL) detaching from a bent fibre ($\theta = 3.9°$). The thin film above the droplet breaks; then the droplet falls from the fibre. The video is recorded at 1000 fps and played back at 1/50 of real time.

SI_video_2.mp4: High speed video of an SDS-water solution droplet (9 µL) detaching from a bent fibre ($\theta = 53.9°$). The droplet slowly slides down along the left side of the fibre. The first 4:00 minutes of the video show the droplet very slowly moving to the left. At 4:20 the droplet begins to detach from the right-hand fibre and quickly moves downward along the left side of the fibre. The video is recorded at 1000 fps and played back at 1/20 of real time.

4 Derivation of model I (free energy approach)

We can develop mathematical models for the aforementioned observations, and start by considering the case of a droplet that wets and is attached to a horizontal fibre (Fig. S6). The total free energy (G) attributed to the droplet on a horizontal fibre at equilibrium is

$$G = H_v \Omega + \gamma A_{LA} + \gamma_{SA} A_{SA} + \gamma_{LS} A_{LS} - \rho g \Omega z, \tag{S1}$$

where H_v is the volumetric free energy of the fluid, g is the gravitational constant, γ is the liquid surface tension, ρ is the density of the fluid, γ_{SA} and γ_{LS} are the interfacial energies at the solid-air interface and the liquid-solid interface, respectively. A_{SA} and A_{LS} are the areas of the solid-air interface and liquid-solid interface, respectively. Ω is the volume of the fluid, and z is the center of mass of the droplet. By assuming that Young's equation ($\gamma \cos\alpha + \gamma_{LS} = \gamma_{SA}$, where α is the wetting angle) valid in this situation, eqn (S1) can be rewritten without the γ_{LS} term:

$$G = H_v \Omega + \gamma A_{LA} + \gamma_{SA} A_{SA} + (\gamma_{SA} - \gamma \cos\alpha) A_{LS} - \rho g \Omega z. \tag{S2}$$

When the position of droplet (z) is perturbed (from z to $z + \delta z$) by a vanishing distance δz (herein, we use "δ" as variational notation; refer to Fig. S6 for the geometric details), there is a change in G (denoted as δG hereafter) which can be used to determine the stability criterion of the droplet-fibre system. Noting that a positive perturbation δz leads to a negative value of δA_{LS} (meaning that the fibre is dewetted when the droplet moves downward), and invoking $\delta A_{SA} = -\delta A_{LS}$, variation of eqn (S2) leads to

$$\delta G = H_v \delta\Omega + \gamma \delta A_{LA} - \gamma \cos\alpha \delta A_{LS} - \rho g \Omega \delta z. \tag{S3}$$

Noting that the droplet maintains a constant volume ($\delta\Omega = 0$) after perturbation, eqn (S3) becomes

$$\delta G = \gamma \delta A_{LA} - \gamma \cos\alpha \delta A_{LS} - \rho g \Omega \delta z, \tag{S4}$$

where the first term on the right hand side is the surface energy contribution from the change in the liquid-air interface area. The second term represents the contribution from the change in the liquid-solid interface area, and the third term is the gravitational energy change under perturbation.

The solid-liquid interface area is $A_{LS} \approx 4\pi b R \cos\beta$ (side surface area of a section of cylindrical fibre ($\overline{AB}$, length $2R\cos\beta$), as shown in Fig. S6), where R is the radius of the droplet when assuming the droplet is spherical, and β is the angle between horizontal and the 3-phase point where the fibre exits the droplet ($\angle BOH$, in Fig. S6). Assuming that the shape of the droplet does not change after an infinitesimal perturbation of δz ($\delta A_{LA} = 0$), the free energy change due to the perturbation can be derived from eqn (S4):

$$\delta G \approx \gamma 4\pi b \sin\beta \delta\beta R \cos\alpha - \rho g \Omega \delta z. \tag{S5}$$

Noting that $R \cos\alpha \delta\beta / \delta z \sim O(1)$ [1], we have the energy potential:

$$\frac{\delta G}{\delta z} \approx \gamma 4\pi b \sin\beta - \rho g \Omega. \tag{S6}$$

[1] See eqn (S10) and corresponding analysis for more details.

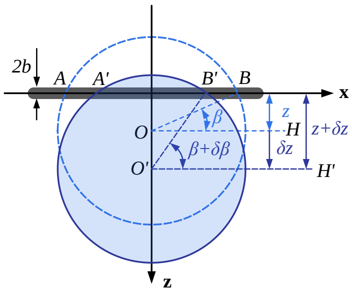

Fig. S6: Geometry of a droplet on a fibre of diameter $2b$. The spherical droplet is originally positioned on a horizontal fibre ($\theta = \pi/2$) at equilibrium (represented by the dashed line with centre O). The position of the droplet moves down to δz when perturbed from equilibrium (represented by the filled circle with centre O'). β is the angle between horizontal and the 3-phase point where the fibre exits the droplet ($\angle BOH$). The solid-liquid contact angle is not drawn.

A critical condition approaches as $\delta G/\delta z \to 0$ and leads to a critical volume of the droplet:

$$\Omega \approx \frac{4\pi\gamma b \sin\beta}{\rho g}. \tag{S7}$$

Defining the capillary length of a fluid as $\lambda = \sqrt{\gamma/\rho g}$, eqn (S7) is identical to the equation ($\sin\beta = \frac{1}{3}\frac{R^3}{b\lambda^2}$) found by Lorenceau *et al.* (2004), which we also validated experimentally. It is worth mentioning that, taking advantage of this energy based analysis, we are able to avoid the "assumed equivalent" configuration (two inclined fibres joining a droplet) used by Lorenceau *et al.* (2004). Instead, we can directly analyze the stability of droplet held by a horizontal fibre. Nevertheless, the two modeling techniques (the energy based method employed in this paper and force balances used in Lorenceau *et al.* (2004)) confirm each other well.

A positive value of $\delta G/\delta z$ means that a droplet resists perturbation and tends to stay on the fibre with certain robustness (e.g., Ω is sufficiently small). At the critical condition ($\delta G/\delta z = 0$), the volume of the droplet is large enough that the contribution from the gravitational potential (negative) tends to dominate over the contribution from interfacial energy (positive) given an infinitesimal perturbation. The destabilized droplet-fibre system then tends to fall off the fibre. On the other hand, when $\delta G/\delta z < 0$ (e.g., Ω is sufficiently large), a droplet falls off immediately due to the negative free energy potential.

Eqn (S7) implies that the maximum possible volume of a liquid held by a horizontal fibre will occur when $\sin\beta$ approaches unity. The maximum droplet size can now be estimated by normalizing eqn (S7) by a characteristic volume of a spherical droplet whose radius is the capillary length ($\tilde{\Omega} = \frac{4}{3}\pi\lambda^3$) yielding:

$$\Omega_I^* = \frac{\Omega}{\tilde{\Omega}} \lesssim 3\frac{b}{\lambda}, \tag{S8}$$

which we label as *model I*. Physical insights based on this model can be found in ESI §7.

Next, we provide a brief auxiliary analysis for model I, where a modified model I is proposed that includes a wetting contact angle (α), and more details about derivation of model I (i.e., eqn (S5)–eqn (S7)) can be found in this section too.

Under a downward perturbation δz, the relative position of the droplet and the horizontal fibre changes and the equivalent geometry is shown in Fig. S7.

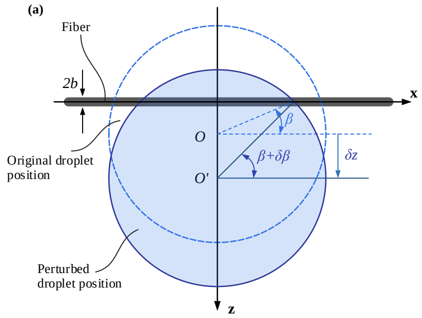

Fig. S7: Physical sketch for model I (left), and the equivalent geometry (right).

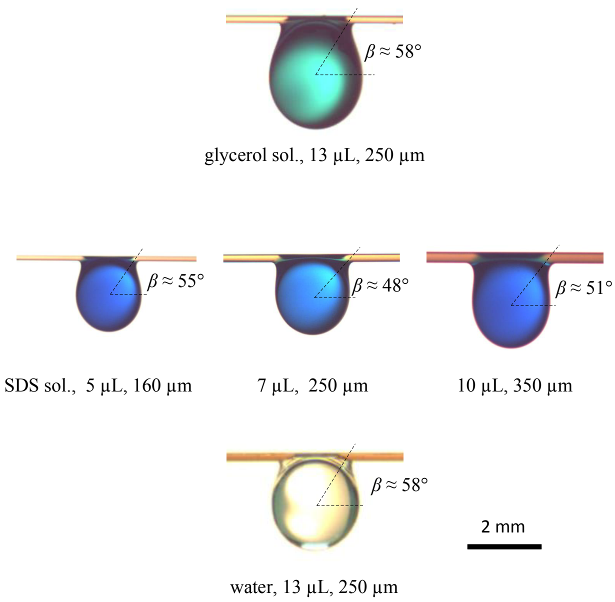

Fig. S8: Measured β at critical conditions for glycerol-water solution (top row), SDS-water solution (middle row), and pure water (bottom row) on horizontal fibres with different diameters and volumes as marked.

Noting that $R\delta\beta$ is the arc length (Fig. S7), it is not hard to find: $R\delta\beta/\delta z \approx \sec\beta$. Invoking eqn (S5), a more complete from of the eqn (S6) can be derived:

$$\frac{\delta G}{\delta z} = \gamma 4\pi b \cos\alpha \tan\beta - \rho g \Omega. \tag{S9}$$

Thus, in the critical condition, $\delta G/\delta z \to 0$ leads to

$$\Omega = \frac{\gamma 4\pi b \sin\beta}{\rho g} \frac{\cos\alpha}{\cos\beta}, \tag{S10}$$

which is a modified form of eqn (1) in the paper, and includes effect of the contact angle α. When $\alpha \geq 90°$, $\cos\alpha \leq 0$, and thus, $\Omega \leq 0$. Physically, this implies that a "hydrophobic" fibre can not hold any liquid.

In our experiments, we noticed that $\cos\alpha/\cos\beta \sim O(1)$ [2], which is equivalent to $R\delta\beta\cos\alpha/\delta z \sim O(1)$ as proposed in the modeling section (ESI §4). Experimental evidence can be found in Fig. S8, and external experimental support can be found in Lorenceau *et al.* (2004). Thus, one arrives at eqn (6) of the paper:

$$\Omega \approx \frac{4\gamma\pi b \sin\beta}{\rho g}.$$

This is identical to the model developed by Lorenceau *et al.* (2004) using a force balance derivation.

[2]For example, at critical condition, β ranges from $\sim 48°$ to $\sim 58°$, and $\cos\beta$ ranges from ~ 0.53 to ~ 0.67. Contact angle α ranges from $\sim 30°$ to $\sim 59°$, and $\cos\beta$ ranges from ~ 0.5 to ~ 0.86.

5 Derivation of model II (free energy approach)

We continue our analysis with the same free energy based technique applied in ESI §4 to the fibre bent at small angles (e.g., $\theta \lesssim 18°$). At small angles, a droplet of critical size is characterized by a triangular thin film connected to the apex of the fibre (Fig. 1(c) in the paper). The area of the liquid-air interface is $A_{LA} \approx 2zL\sin\theta$, and the area of the liquid-solid interface is $A_{LS} \approx 4\pi bL$ (Fig. S9). Noting $z \approx L$ and $\sin\theta \approx \theta$ when θ is small, analysis of eqn (S4) indicates that given an infinitesimal perturbation on the position of the droplet (δz) the free energy change of the droplet is

$$\delta G \approx \gamma(4z\theta - 4\pi b\cos\alpha)\delta z - \rho g\Omega\delta z. \tag{S11}$$

Our experiments show that in this regime, generally, the width of the bottom of the droplet ($2ztan\theta \approx 2z\theta$) is significantly larger than the diameter of the fibre ($2b$) (Fig. 1(c) in the paper). In other words, the contribution to δG from the fibre thickness is negligible compared to that of the liquid film between the fibre.

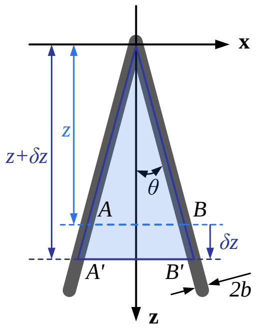

Fig. S9: Geometry of a droplet between a bent fibre (diameter $2b$) with small θ. The bottom of the droplet (solid line, $A'B'$) moved δz downward after a perturbation from the original position (dashed line, AB). The solid-liquid contact angle is not drawn.

The critical state is approached as $\delta G/\delta z \to 0$ and leads to a critical volume of the droplet at small angles:

$$\Omega \approx 4\gamma L\theta/\rho g. \tag{S12}$$

Again, when $\delta G/\delta z < 0$, the droplet total energy is reduced by perturbation and the droplet subsequently falls. Normalizing eqn (S12) with characteristic volume ($\tilde{\Omega}$), we have created *model II* that describes the critical volume for small angles:

$$\Omega^*_{II} = \frac{\Omega}{\tilde{\Omega}} \approx \frac{3L}{\pi\lambda}\theta = \frac{3}{\pi}L_0\theta, \tag{S13}$$

where $L_0 = L/\lambda$ is a length scale that characterizes the wetted length compared to the capillary length. Physical insights based on this model can be found in ESI §7. An alternative derivation of model II based on a force balance (similar to the method used in Lorenceau *et al.* (2004)) can be found in ESI §6.

6 Alternative derivation of model II (force balance approach)

In this section, we provide an alternative derivation of model II based on force balances analysis. As shown in Fig. S10, the weight of the droplet ($\Omega\rho g$) is balanced by vertical projection of the capillary forces ($2\kappa\gamma L$) on the fibre, thus, we have

$$\Omega\rho g = 4\kappa\gamma L \sin\theta,$$

where, $\kappa = \int_0^L \cos\varphi(\xi)d\xi/L$ is a variable that measures the space averaged effects of the local contact angle ($\varphi(\xi)$) formed at the interface of the thick film of the droplet and the fibre (see the local cross-section A-A of Fig. S10). Noting that the when θ is small, the local contact angle $\varphi(\xi)$ is small (e.g., see the droplet morphology shown in Fig. 1(c), or the first row in Fig. S3), it is reasonable to assume $\varphi(\xi) \approx 0$ for a considerably large portion along the fibre length (ξ), and thus, $\kappa \approx 1$. Invoking $\theta \approx \sin\theta$ when $\theta \to 0$, we arrive at $\Omega\rho g \approx 4\gamma L\theta$, or

$$\Omega \approx \frac{4\gamma L\theta}{\rho g},$$

which is identical to eqn (3) in the paper (model II).

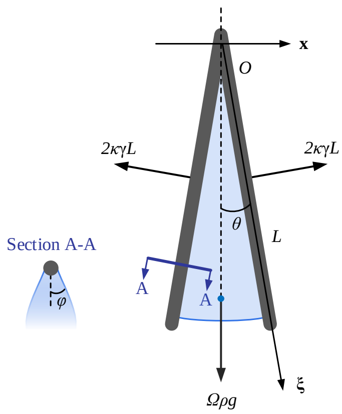

Fig. S10: Free body diagram of the force balance on a droplet. L is the wetted length of one side of the fibre bent at an angle θ at the origin O. The capillary force is represented by ΩgL and ξ represents the axis of the fibre. A-A is a line indicating where the cross-section cutaway perpendicular to the fibre was made. The view of this local cutaway is shown as Section A-A. φ is the local contact angle of the droplet on the fibre.

7 Physical interpretation of models I & II

It is worth noting that the free energy based derivation of model I and II itself allows access to more physical insights explicitly. These physical interpretations are not directly offered by force balance analysis, despite that force balances are seemingly more straightforward (see ESI §6 and the modeling technique in Lorenceau *et al.* (2004)).

Starting with one governing equation eqn (S4), we arrived at two models (model I, associated with eqn (S7) and model II, associated with eqn (S12), respectively) by introducing two different assumptions. For example, eqn (S7) is derived by assuming that the droplet shape remains the same under perturbation; thus, the area of the liquid-air interface (A_{LA}) remains constant ($\delta A_{LA} \approx 0$, meaning that the *first* term on the right hand side of eqn (S4) is neglected, denoted as *assumption I*). To arrive at eqn (S12), we assumed that $\delta A_{LS} \approx 0$ (*assumption II*), meaning that the contribution from the change in solid-liquid interfacial area (δA_{LS}) is negligible compared to the contribution from the liquid-air interface (δA_{LA}) when the droplet is perturbed. In other words, the *second* term of the right hand side of eqn (S4) vanishes. This mathematical symmetry provides explicit physical meaning for the models of regimes I and II. There is “competition” between the contributions of liquid-air interface and liquid-solid interface: when $\theta \to 0$, the liquid-air interface A_{LA} is the dominant factor of the stability of the droplet-fibre system. On the other hand, the physics of a droplet attached on a horizontal fibre ($\theta = \pi/2$) is dominated by the liquid-solid interface A_{LS}. In regime III, between these extremes, we propose that upon perturbation, neither the droplets shape (δA_{LA}) nor the wetted area (δA_{LS}) remain constant.

8 Stability analysis on a slightly bent fibre (transition from region I to region III)

In this section we investigate the stability of a droplet on a slightly bent fibre ($\theta \lesssim \pi/2$) to examine the transition from region I ($\theta = \pi/2$) to region III ($\theta < \pi/2$).

Starting with eqn (S4), neglecting the contribution from the changes in droplet shape (δA_{LA}), we have

$$\frac{\delta G}{\delta z} = -\gamma \cos\alpha \frac{\delta A_{LS}}{\delta z} - \rho g \Omega. \tag{S14}$$

Note that $\delta A_{LS} = -4\pi b \delta L$, where δL is the de-wetted length of the fibre (Fig. S11), the critical volume of a droplet can be reached by letting $\delta G/\delta z \to 0$:

$$\Omega = \frac{4\pi\gamma b \cos\alpha}{\rho g} \frac{\delta L}{\delta z}.$$

Based on the law of sines (see Fig. S11 for the trigonometry), we have

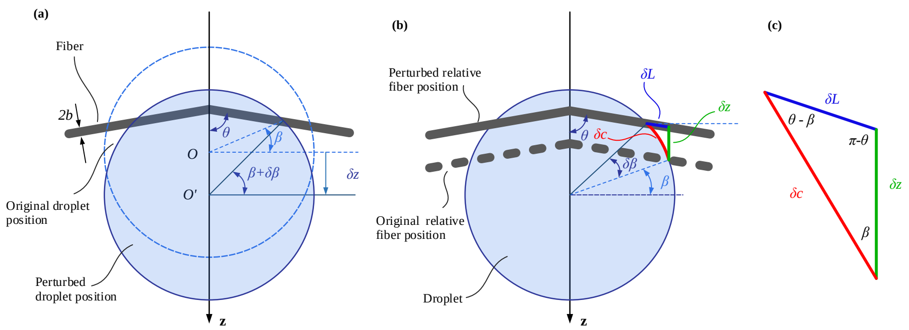

Fig. S11: Physical sketch for a droplet held by a slightly bent fibre under perturbation (a), the equivalent geometry (b), and the geometry of the corresponding analysis (c).

$$\frac{\delta z}{\sin(\theta - \beta)} = \frac{\delta L}{\sin\beta}. \tag{S15}$$

Note that for a slightly bent fibre ($\theta \lesssim \pi/2$), $\cos\theta \approx 0$ and $\sin\theta \approx 1$. The above law of sines can be rewritten as

$$\frac{\delta L}{\delta z} \approx \frac{\sin\beta}{\cos\beta \sin\theta}. \tag{S16}$$

Combining above, the critical volume is

$$\Omega \approx \frac{4\pi\gamma b}{\rho g} \frac{\cos\alpha}{\cos\beta} \frac{\sin\beta}{\sin\theta}. \tag{S17}$$

This equation has the same form as eqn (7) in the paper, meaning that

$$\text{Volume} = \text{fn}(\theta) = \frac{\text{Capilary Force}}{\text{Specific Weight}} \frac{1}{\sin\theta}.$$

In the limit of $\theta \to \pi/2$, recalling that $\cos\alpha/\cos\beta \sim O(1)$ [3] and $\sin\theta \to 1$, this equation becomes eqn (1) of the paper. Thus, there is not necessarily a discontinuity at the boundary of Region I and Region III. Experimental evidence found in Fig. 1 or Fig. 5 in the paper suggests a reasonably smooth transition.

[3] See Fig S7 and corresponding analysis in ESI §4 for more details and external experimental supports can be found in Lorenceau *et al.* (2004).

9 An alternative model for regime III

For angles $18^\circ \lesssim \theta \lesssim 90^\circ$, we consider the force balance between the gravitational component and the surface tension provided by one side of the fibre (Fig. S12) under perturbation. The experimental observations reveal that at these angles a droplet slides down along one side of the fibre during detachment (Fig. 3 in the paper or SI video 2). Thus we can formulate the balance as

$$\rho g \Omega \sin\theta = 2\kappa\gamma L, \tag{S18}$$

where $\kappa = \int_0^L \cos\varphi(\xi)\mathrm{d}\xi/L$ is a variable that measures the space-averaged effects of the local contact angle ($\varphi(\xi)$) formed at the interface of the thick film of the droplet and the fibre as illustrated in the cross-section A-A of Fig. S12).

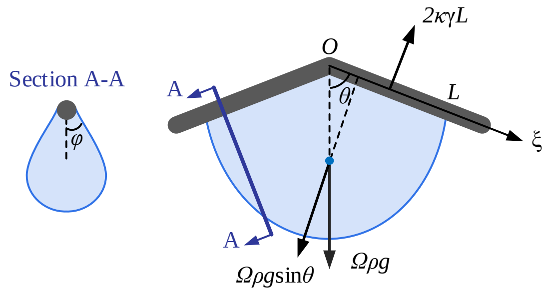

Fig. S12: Free body diagram of the force balance on a droplet. L is the wetted length of one side of the fibre bent at a half angle θ at the origin O. The capillary force is represented by γL and ξ represents the axis of the fibre. A-A is a line indicating where the cross-section cutaway perpendicular to the fibre was made. The view of this cutaway is shown as Section A-A . φ is the local "contact" angle of the droplet.

The droplet profile varies along the fibre as seen in Fig. 3 (ξ-axis of Fig. S12), Accordingly, φ also varies along the fibre, and may even be a complicated function of θ. Thus, κ is difficult to calculate or measure, especially at critical states. However, κ is not a practical or "useful" parameter even if it was a known parameter. Rather, there is no disadvantage to assuming that κ is a constant which may lead to an acceptable and practical fitting parameter that is significantly less complex.

Recalling the the definition of capillary length, and substituting the empirical model of the wetting length eqn (5) into eqn (S18) leads to

$$\Omega \approx \kappa \frac{2\lambda^3}{\sin^2\theta}. \tag{S19}$$

By choosing a simple κ value $\kappa \approx 0.5$ we see decent agreement with the experiment especially when θ is relatively large. Normalizing the droplet volume by the characteristic volume ($\tilde{\Omega}$) leads to an alternative semi-analytical model for regime III (*model III′*):

$$\Omega^*_{III'} = \frac{\Omega}{\tilde{\Omega}} \approx \frac{3\kappa}{2\pi\sin^2\theta}. \tag{S20}$$

One heuristic way to think about the physical nature of regime III is to consider a spherical droplet with a horizontal fibre running through it. If the fibre is then bent inside the droplet with some small angle ($\theta < \pi/2$ in this case), then the wetted length of the fibre will become $2L/\sin\theta > 2L$ and there will be a larger force attaching the droplet to the longer fibre, so the mass and the volume of the droplet can increase by $\sim 1/\sin\theta$. Recalling that $L \sim \lambda/\sin\theta$, we expect $\Omega^* \sim 1/\sin^2\theta$.

Comparing eqn (4) in the paper and with eqn (S20) to eliminate Ω^* and noticing that $\sin\theta \approx \theta$ for relatively small angles, the angle for maximum droplet volume becomes

$$\theta_{opt} \approx \sin^{-1}\left(\frac{\kappa}{2L_0}\right)^{1/3} \approx 21^\circ. \tag{S21}$$

A comparison of model III (eqn 6 in the paper), and model III′ (eqn (S20)) can be found in Fig. S13. Both the models give reasonable accurate prediction of the optimal angle.

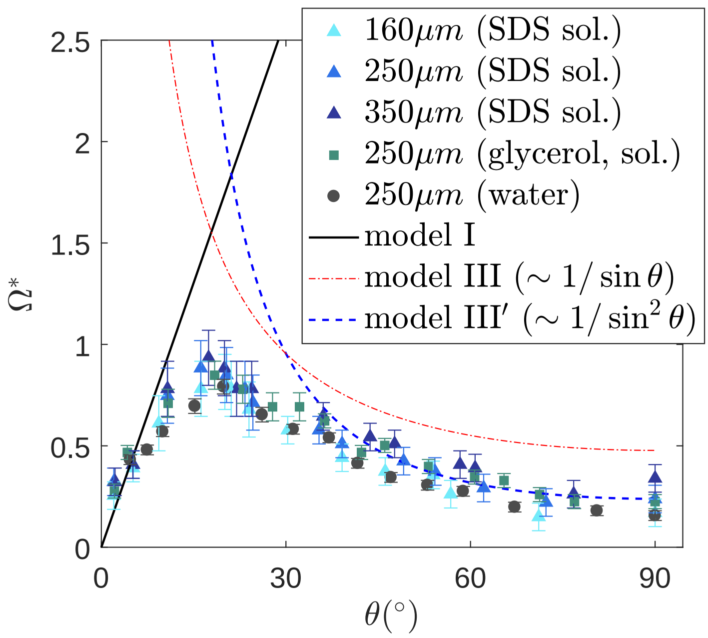

Fig. S13: Comparison of model III and model III′ against experimental data on "θ-Ω^*" plane.

References

É. Lorenceau, C. Clanet and D. Quéré, *Journal of colloid and interface science*, 2004, **279**, 192–197.